Atmospheric
Measurement
Techniques
Open Access
Discussions

An introduction to FY3 GNOS instrument and its performace tested on ground

W. Bai[1], Y. Sun[1], Q. Du[1], G. Yang[2], Z. Yang[2], P. Zhang[2], Y. Bi[2], X. Wang[1], C. Cheng[3], and Y. Han[4]

[1]Center for Space Science and Applied Research, Chinese Academy of Sciences, Beijing, China
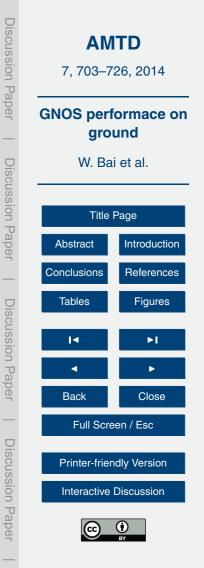[2]National Satellite Meteorological Center, Beijing, China
[3]State Intellectual Property Office of The P.R.C, Beijing, China
[4]Beijing Institute of Petrochemical Technology, Beijing, China

Correspondence to: W. Bai (bjbwh@163.com)

AMTD

7, 703–726, 2014

GNOS performace on ground

W. Bai et al.

Title Page

Abstract	Introduction
Conclusions	References
Tables	Figures

◄◄ | ►►

◄ | ►

Back | Close

Full Screen / Esc
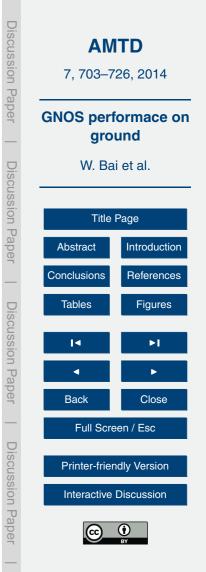
Printer-friendly Version

Interactive Discussion

Abstract

The FY3 GNOS (GNSS Occultation Sounder) mission is a GNSS (Global Navigation Satellite System) radio occultation mission of China for remote sensing of Earth's neutral atmosphere and the ionosphere. GNOS will use both the Global Positioning System (GPS) and the Beidou navigation satellite systems on the China Feng-Yun-3 (FY3) series satellites. The first FY3-C was launched at 03:03 UTC, 23 September 2013. GNOS was developed by Center for Space Science and Applied Research, Chinese Academy of Sciences (CSSAR). It will provide vertical profiles of atmospheric temperature, pressure, and humidity, as well as ionospheric electron density profiles on a global basis. These data will be used for numerical weather prediction, climate research, and ionospheric research and space weather. This paper describes the FY3 GNOS mission and the GNOS instrument characteristics. It presents simulation results of the number and distribution of GNOS occultation events with the Regional Beidou constellation and the full GPS constellation, under the limitation of the GNOS instrument occultation channel number. This paper presents the instrument performance as derived from analysis of measurement data in laboratory and mountain-based occultation validation experiments at Mt. Wuling in Hebei Province. The mountain-based GNSS occultation validation tests show that GNOS can acquire or track lower elevation radio signal for rising or setting occultation events. The refractivity profiles of GNOS obtained during the mountain-based experiment were compared with those from radiosondes. The results show that the refractivity profiles obtained by GNOS are consistent with those from the radiosonde. The RMS of the differences between the GNOS and radiosonde refractivities is less than 3 %.

1 Introduction

When a receiver on-board a low Earth orbiting (LEO) spacecraft tracks a Global Navigation Satellite System (GNSS) satellite in higher orbit as it sets or rises through

Earth's atmosphere, a radio occultation (RO) occurs. The recorded phase and amplitude of the radio waves during the occultation can be analyzed to produce neutral atmospheric (stratosphere and troposphere) parameters, including refractivity, density, pressure, temperature, and humidity, as well as ionospheric Total Electron Content (TEC), refractivity and electronic density profiles.

Application of the RO technique was first used to sound planetary atmospheres beginning in the 1960s (Fishbach et al., 1965; Tyler, 1987; Lusignan et al., 1969). The first demonstration of RO for Earth's atmosphere was the GPS/MET experiment led by the University Corporation of Atmospheric Research (UCAR), which was equipped with the NASA/JPL Turbo-Rogue GPS receiver modified to acquire and track occultation signals (Ware et al., 1996). The success of GPS/MET led to the inclusion of "Black-Jack" GPS RO receivers on the German Challenging Mini-Satellite Payload (CHAMP) (Wickert et al., 2001), Satélite de Aplicaciones Cientificas-C (SAC-C) (Hajj et al., 2004) satellites in 2000, and the twin, co-orbiting satellites of Gravity Recovery and Climate Experiment (GRACE) (Kang et al., 2003) in 2002.
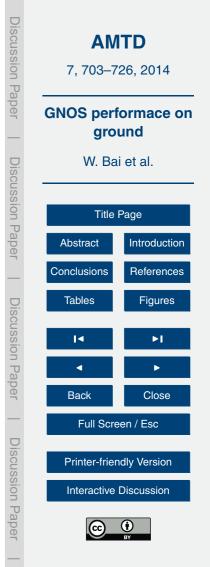
The six-satellite Constellation Observing System for Meteorology, Ionosphere and Climate (FORMOSAT-3/COSMIC), was launched on 15 April 2006. After full deployment and achieving a uniform 30-degree separation of the six orbit planes at the end of 2007, FORMOSAT-3/COSMIC provided about 2500 occultations per day, evenly distributed in local solar time. A distinctive feature of FORMOSAT-3/COSMIC is routine tracking of RO signals in the lower troposphere in open-loop mode, which allows retrieval of the bending angle and refractivity profiles almost down to the surface by application of radio holographic inversion methods (Sokolovskiy et al., 2007; Anthes et al., 2008).

The meteorological satellite Metop-A, launched in 2006, is the one of three EUMETSAT satellites within European Polar System (EPS). The EPS will provide over 14 yr of continuous meteorological observations, including radio occultation (RO) measurements from the GNSS receiver for atmospheric sounding (GRAS). The GRAS

instrument on the Metop-A satellite provides more than 600 radio occultation measurement profiles per day (Bonnedal et al., 2010; Gorbunov and Lauritsen et al., 2006).

The GNSS RO occultation technique has a number of advantageous characteristics for atmospheric remote sensing: self-calibrating, high vertical resolution, precise, long-term stability, all-weather capability and low-cost instrument development (Gleason and Gebre-Egiabher, 2009; Anthes et al., 2008). It has been proven that the RO technique is valuable for the study of the atmosphere, especially, for numerical weather prediction, climate, and ionospheric research and space weather. Therefore, with growing demands for weather and climate information for disaster prevention and reduction, climate change response, ecosystems management, agriculture and forecasting, it is important that the Chinese Feng-Yun (FY) series satellites add the GNSS occultation instrument to contribute to the global observing system.

The GNOS mission (Bi et al., 2012) consists of a GNSS radio occultation explorer for remote sensing of both the Earth's neutral atmosphere and ionosphere, on China's FengYun-3 (FY3) 02 series satellites. The first of this series, FY3-C, was launched at 03:07 UTC, 23 September 2013. The GNOS instrument was developed by Center for Space Science and Applied Research, Chinese Academy of Sciences (CSSAR). A distinctive feature of GNOS is that it is capable of using both the Beidou and GPS navigation satellite systems to provide radio occultation measurements of the atmosphere.

This paper provides a basic introduction to the GNOS instrument. In addition, it shows some simulation results of GNOS occultation events using the Regional Beidou and GPS constellations. Finally, we present the instrument performance as derived from analysis of measurement data in the laboratory and mountain-based occultation validation experiment.

GNOS performace on ground

W. Bai et al.

Title Page

Abstract | Introduction

Conclusions | References

Tables | Figures

◄ | ►

◄ | ►

Back | Close

Full Screen / Esc

Printer-friendly Version

Interactive Discussion

2   The GNOS instrument

The GNOS instrument consists of three antennas, the Positioning Antenna (PA), the Rising Occultation Antenna (ROA), and the Setting Occultation Antenna (SOA) in physical structure or five antennas, the PA, the Rising Ionosphere Occultation An-
5   tenna (RIOA), the Setting Ionosphere Occultation Antenna (SIOA), the Rising Atmosphere Occultation Antenna (RAOA), and the Setting Atmosphere Occultation Antenna (SAOA) in electrical structure. There are three RF Units (RFUs) and one GNSS Electronics Unit (EU). Each antenna is connected to its RFU with sharp cavity filters, which are placed close to the antennas to protect the GNOS from the complex RF environ-
10   ment onboard FY3-C. Each RFU is connected to the EU. A photograph of the instrument is shown in Fig. 1.

The PA is a wide beam with hemispherical coverage, low-gain antenna pointing at zenith. The GNOS instrument is capable of tracking up to six Beidou satellites and more than eight GPS satellites through this antenna. These measurements are used
15   for real-time navigation, positioning as well as for precise orbit determination through post-processing on the ground.

The along-velocity viewing antenna ROA (including RIOA and RAOA) and anti-velocity viewing antennas SOA (including SIOA and SAOA) are used for rising and setting occultation tracking. The GNOS has the capability of tracking up to four Bei-
20   dou and six GPS occultations simultaneously. The atmosphere occultation antennas (including RAOA and SAOA) have a pattern that is wide in azimuth and narrow in elevation. A gain of approximate 10 dBi is reached over the coverage range between +35 and −35° in azimuth and from +7.5 to −7.5° in elevation.

The EU of GNOS is based on a Field Programmable Gate Array (FPGA) + Digital
25   Signal Processor (DSP) Framework. After filtering and down-conversion in the RFU, the signals are digitally down converted with Analog to Digital Converter (ADC), then sampled at a high rate and transmitted to the channel processor of the EU, where the GNOS accomplishes navigation, positioning and occulting GNSS satellite prediction

and selection, signal acquisition and tracking, and data handling. An Ultra Stable Oscillator (USO) is used as a reference oscillator with very stable frequency (1 s Allan variance of 10^{-12}) in order to retrieve atmospheric measurements with high accuracy. It also allows us to using zero-difference method to invert the excess phase measure-
ments (Beyerle et al., 2005).

GNOS is a multi-frequency receiver with Beidou/GPS compatibility, B1/B2 closed-loop (CL) tracking, GPS L2 codeless-mode operating for P code, GPS L2C closed-loop tracking and GPS L1 C/A closed-loop and open-loop (OL) tracking capabilities. The Beidou and GPS compatible instrument increases the number of transmitting
sources and promises significant enhancements in throughput of the measurements. A multi-frequency operating instrument is needed for ionosphere parameters retrieval and ionospheric correction in pre-processing of atmospheric parameters. The receiver measures the following observable parameters for each tracked GPS and Beidou satellite: (1) L1 C/A-code phase, (2) L1 carrier phase, (3) L1 signal amplitude, (4) L2 P-code
phase, (5) L2 C/A-code phase (if present), (6) L2 carrier phase, (7) L2 signal amplitude, (8) B1 C/A-code phase, (9) B1 carrier phase, (10) B1 signal amplitude, (11) B2 C/A-code phase, (12) B2 carrier phase, (13) B2 signal amplitude.

In the lower part of the troposphere where highly dynamic signal conditions are frequently encountered due to the strong atmospheric modulation, the GPS L1 signal
is tracked in open loop in parallel to the closed loop tracking. In open-loop tracking, the signal is down-converted using a numerically controlled oscillator, which generates a frequency given by an onboard Doppler model pre-calculated in GNOS without a feedback from received signal (Sokolovsky, 2001; Sokolovsky et al.). Particularly, for the rising occultation, an a priori range model of the atmospheric delay (Ao et al., 2009)
is also calculated onboard the GNOS. The baseband signal is then sampled at a rate of 100 kHz. Furthermore, a sample rate of 100 Hz of open-loop tracking is proved to be sufficient to capture the signal modulated by the atmosphere dynamics and uncertainties of the Doppler model (Bonnedal et al., 2010).

The design specifications of GNOS are summarized in Table 1; it can be seen that some parameters of the FY3 GNOS are comparable to those of COSMIC (Rocken et al., 2000) or Metop/GRAS (Loiselet et al., 2000).

The mass for the whole GNOS instrument is around 14 kg. The power consumption in full operation (Beidou and GPS, navigation and occultation) is about 40 W. The average GNOS data rate is 86 kbit s^{-1}, with peaks of up to 170 kbit s^{-1}. The characteristics of GNOS are displayed in Table 2.

3   GNOS occultation events simulation

The Chinese FY3 weather satellites will be in sun-synchronous orbits with an altitude of 836 km and inclination of 98.75°. Knowing the key parameters of FY3-C, we can simulate its orbit. A regional Beidou (China Satellite Navigation Office, 2012) constellation of 14 (5GEO+5IGSO+4MEO) satellites and a full GPS constellation of 32 satellites acting as transmitter system were assumed. The simulation period was 24 h. With the limitation of the GNOS instrument occultation channel number described in Table 1 and the occultation antenna coverage range in azimuth (+35 deg to −35 deg), a total of 696 occultation events, including 192 (98 risings + 94 settings) Beidou occultation events and 534 (268 risings + 266 settings) GPS occultation events can be obtained. The global distribution for all simulated occultation events for Beidu and GPS are shown in Figs. 2 and 3, respectively.

4   GNOS performance testing and analysis on ground

4.1   Laboratory tests

Important performance characteristics for a user of RO measurements are the code and carrier phase measurements precision and real-time navigation precision. These properties were analyzed in the lab.
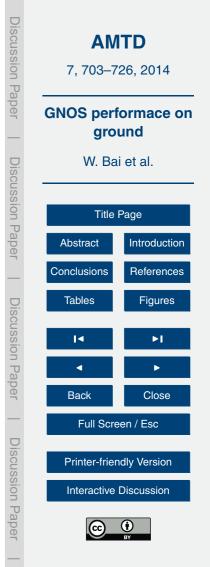
The tests employed for the GNOS measurements performance study were conducted on Beidou and GPS signal simulators, which allow for a realistic modeling of a space-borne FY3-C user trajectory. The "Virtual" Zero Baseline test (VZB) method (Oliver et al., 2006) was adopted to measure the precision of the observations, which was designed to require only a single receiver unit. A week-long consecutive test was carried out with a simulator output signal power level of −123 dBm for GPS L1C/A, Beidou B1 and B2, −126 dBm for GPS L2C/A and −129 dBm for GPS L2P. The results showed that the pseudorange measurement precision was less than 17 cm for Beidou B1(SNR = 48 dB), less than 30 cm for Beidou B2(SNR = 48 dB), less than 16 cm for GPS (L1C/A SNR = 48 dB, L2C/A SNR = 45 dB, L2P SNR = 33 dB). And the carrier phase measurement precision was less than 1.2 mm for both the Beidou and GPS. The noise properties of code and carrier phase measurements lasting about 700 s are shown in Figs. 4 and 5 for Beidou and GPS.

In addition, during the test in lab based on GNSS simulator, we also estimated the precision of navigation in real-time by comparison GNOS real-time positioning results with the simulation values. The navigation errors were less than 3 m for Beidou in three dimensions of WGS84 coordinates, and less than 1 m for GPS. The noise properties of the navigation measurements lasting about 700 s are shown in Fig. 6.

4.2 GNOS performance testing in mountain-based validation experiment

A GNOS validation experiment was performed in collaboration with National Meteorological Administration of China (CMA) on the top of Mt. Wuling from 13 to 28 September 2011 in order to obtain atmosphere parameter profiles near the Earth's surface and validate the performance of GNOS prototype before its launch. However, in that period the Beidou constellation was not operating, so we focused on GPS occultation testing.

The GNOS occultation antenna was installed in the roof of a hotel on the top of Mt. Wuling located at an altitude of about 2038 m. The southward view gives the best unobstructed view of the horizon. The GNOS prototype receiver and the computer were

GNOS performace on ground

W. Bai et al.

placed inside the hotel. The antenna and receiver were connected by cable with length of 20 m.

During the observation period, an average of about 20 GPS occultation events were observed daily. Details of the observation statistics in occultation events number distribution in azimuth are given in Fig. 7, including 80 events in 18–21 September. Most of the valid occultations occurred viewing toward the south (180°).

The single-differencing procedure was adopted to generate atmospheric excess phase. It required the receiver receiving an occulting GNSS satellite and a non-occulting reference GNSS satellite signals simultaneously. The occultation link (GNOS-GNSS_occ) and reference link (GNOS-GNSS_ref) data were differenced to remove receiver clock errors. The GNSS (GPS) transmitter clock errors were then eliminated based on the IGS final clock products. After the carrier phase correction of the position difference between the occultation and positioning antennas, we obtained the excess phase. Assuming local spherical symmetry, partial bending angle $\alpha'(a)$ (Healy, 2002; Hu, 2006), subtracting the positive elevation bending angle $\alpha_P(a)$ from the negative bending angle $\alpha_N(a)$ with the same impact parameter a, was given

$$\alpha'(a) = \alpha_N(a) - \alpha_P(a) \tag{1}$$

Along the section of path below the receiver, the Abel formula can be used to describe the relationship between the partial bending angle and the atmospheric refractive index as

$$\alpha'(a) = -2a \int_{a}^{n_R r_R} \frac{\mathrm{d}\ln n/\mathrm{d}x}{(x^2 - a^2)^{1/2}} \mathrm{d}x \tag{2}$$

Where $\alpha'(a)$ is the ray partial bending angle, a is the impact parameter, n is refractive index below the altitude of the receiver, n_R is the refractive index at the receiver, and

r_R is the radius of the receiver. Equation (2) can be inverted with

$$n(x) = n_R \exp\left(\frac{1}{\pi} \int_x^{n_R r_R} \frac{\alpha'(a)}{(a^2 - x^2)^{1/2}} \mathrm{d}a \right) \qquad (3)$$

Using the processing described above. We succeeded in retrieving the refractivity profiles over the south area of Mt. Wuling from CL and OL measurement data. These profiles were consistent with radiosonde observations near Mt. Wuling (about 100 km south of the experiment site). The radiosonde data were downloaded from the NOAA radiosonde website. For example, differences in one occultation event between retrieved profiles and nearby radiosonde profiles within one hour are shown in Fig. 8.

We found 15 pairs of GNOS and radiosonde data whose time interval were less than one hour. The RMS difference between the GNOS and radiosonde was 2.88 % in GNOS closed-loop (CL) tracking results and 2.75 % in GNOS open-loop (OL) tracking results. Moreover, GNOS OL tracked longer in time of duration and lower in elevation than CL tracking. The lowest tracked elevation of occultation events was −2.99° in CL and −3.36° in OL. In conclusion, GNOS OL performed better than CL, and the statistical result shows that RMS of the relative difference between the GNOS and radiosonde is less than 3 %.

In addition, we also carried out a complementary mountain-based validation experiment in same place in 20–27 September 2012, in order to test the capability of GNOS to track the Beidou system. However, at that time Beidou did not provide regional services formally. About 2 MEO occultation events were observed daily without precise ephemeris, so we just carried out a GNOS Beidou occultation functional test. Figure 9 shows the first refractivity profile retrieved by Beidou MEO satellite occultation measurements (PRN = 12) as well as a GPS occultation event (PRN = 14) that took place within half an hour. The GNOS refractivity profiles from the Beidou and GPS satellites show basic agreement.

5 Conclusions

The GNOS (GNSS Occultation Sounder) is a new generation instrument for the Chinese FY series meteorological satellites for radio occultation sounding of Earth's neutral atmosphere and ionosphere. The GNOS observations will substantially contribute to the global observing system by providing accurate and precise radio occultation soundings in all-weather conditions. GNOS was designed for observing setting and rising occultation from both the Beidou and GPS navigation satellite constellations.

We performed measurements in closed-loop (CL) and open-loop (OL) modes, similar to COSMIC and METOP. The results show that the GNOS instrument provides more than 500 GPS occultations plus about 200 Beidou occultations per day. The performance of the GNOS instrument in laboratory tests was found to agree with requirements of the GNOS instrument. In mountain-based experiments, the refractivity profiles of GNOS from GPS and Beidou were compared with those of nearby radiosonde data within one hour. The comparison showed that the refractivity profiles obtained by GNOS were consistent with those of the radiosonde. The RMS difference between the GNOS and radiosonde was less than 3 %.

References

Anthes, R. A., Bernhardt, P. A., Chen, Y., Cucurull, L., Dymond, K. F, Ector, D., Healy, S. B., Ho, S.-P., Hunt, D. C., Kuo, Y.-H., Liu, H., Manning, K., McCormick, C., Meehan, T. K., Randel, W. J., Rocken, C., Schreiner, W. S., Sokolovskiy, S. V., Syndergaard, S., Thomp-

son, D. C., Trenberth, K. E., Wee, T.-K., Yen, N. L., and Zeng, Z.: The COSMIC/FORMOSAT-3 mission: early results, B. Am. Meteorol. Soc., 89, 313–333, 2008.

Ao, C. O., Hajj, G. A., Meehan, T. K., Dong, D., Iijima, B. A., Mannucci, A. J., and Kursinski, E. R.: Rising and setting GPS occultations by use of open-loop tracking, J. Geophys. Res., 114, D04101, doi:10.1029/2008jd010483, 2009.

Beyerle, G., Schmidt, T., Michalak, G., Heise, S., Wickert, J., and Reigber, C.: GPS radio occultation with GRACE: atmospheric profiling utilizing the zero difference technique, Geophys. Res. Lett., 32, L13806, doi:10.1029/2005GL023109, 2005.

Bi, Y.-M., Yang, Z.-D., Zhang, P., Sun, Y.-Q., Bai, W.-H., Du, Q.-F., Yang, G. L., Chen, J., and Liao, M.: An introduction to China FY3 radio occultation mission and its measurement simulation, Adv. Space Res., 49, 1191–1197, doi:10.1016/j.asr.2012.01.014, 2012.

Bonnedal, M., Christensen, J., Carlstroem, A., and Berg, A.: Metop-GRAS in-orbit instrument performance, GPS Solut., 14, 109–120, doi:10.1007/s10291-009-0142-3, 2010.

China Satellite Navigation Office: Beidou navigation satellite system signal in space interface control document-open service signal B1I(V 1.0), 2012.

Fjeldbo, G., Kliore, A. K., and Eshleman, V. R.: The neutral atmosphere of Venus as studied with the Mariner V radio occultation experiments, Astron. J., 76, 123–140, 1971.

Gleason, S. and Gebre-Egiabhet, D.: GNSS Applications and Methods, London, ARTECH HOUSE Press, London, 530 pp., 2009.

Gorbunov, M. E., Lauritsen, K. B., Benzon, H.-H., Larsen, G. B., Syndergaard, S., and Sørensen, M. B.: Processing of GRAS/METOP radio occultation data recorded in closed-loop and raw-sampling modes, Atmos. Meas. Tech., 4, 1021–1026, doi:10.5194/amt-4-1021-2011, 2011.
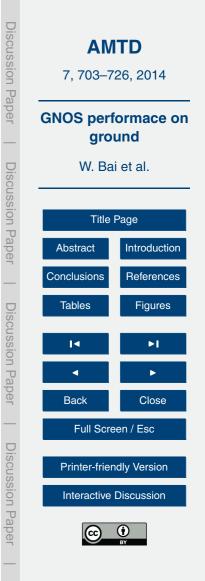
Hajj, G. A., Ao, C. O., Iijima, B. A., Kuang, D., Kursinski, E. R., Mannucci, A. J., Meehan, T. K., Romans, L. J., de la Torre Juarez, M., and Yunck, T. P.: CHAMP and SAC-C atmospheric occultation results and intercomparisons, J. Geophys. Res., 109, D06109, doi:10.1029/2003JD003909, 2004.

Healy, S. B., Haase, J., and Lesne, O.: *Letter to the Editor* Abel transform inversion of radio occultation measurements made with a receiver inside the Earth's atmosphere, Ann. Geophys., 20, 1253–1256, doi:10.5194/angeo-20-1253-2002, 2002.

Hu, X., Zhang, X.-X., Wu, X.-C., Xiao, C.-Y., Zeng, Zeng, Gong, X.-Y.: Mountain-based GPS occultation observations and its inversion theory, Chinese J. Geophys.-Ch., 49, 15–21, 2006.

Kang, Z., Nagel, P., and Pastor, R.: Precise orbit determination for GRACE, Adv. Space Res., 31, 1875–1881, 2003.

Loiselet, M., Stricker, N., Menard, Y., and Luntama, J.-P.: GRAS – Metop's GPS-based atmospheric sounder, ESA Bull.-Eur. Space, 102, 38–44, 2000.

Lusignan, B., Modrell, G., Morrison, A., and Pomalaza, J.: Sensing the Earth's atmosphere with occultation satellites, P. IEEE, 57, 458–467, 1969.

Oliver, M., Miquel, G.-F., and Jacob, W.: Performance comparison of semicodeless GPS receivers for LEO satellites, GPS Solut., 10, 249–261, 2006.

Rocken, C., Kuo, Y.-H., Schreiner, W., Hunt, D. C., and Sokolovskiy, S. V.: COSMIC system description, Terr. Atmos. Ocean. Sci., 11, 21–52, 2000.

Sokolovskiy, S.: Tracking tropospheric radio occultation signals from low Earth orbit, Radio Sci., 36, 483–498, 2001.

Sokolovskiy, S. V., Rocken, C., Lenschow, D. H., Kuo, Y. - H., Anthes, R. A., Schreiner, W. S., and Hunt, D. C.: Observing the moist troposphere with radio occultation signals from COSMIC, Geophys. Res. Lett., 34, L18802, doi:10.1029/2007GL030458, 2007.

Sokolovskiy, S., Rocken, C., Schreiner, W., Hunt, D. C., and Johnson, J.: Postprocessing of L1 GPS radio occultation signals recorded in open-loop mode, Radio Sci., 44, RS2002, doi:10.1029/2008RS003907, 2009.

Tyler, G. L.: Radio occultation experiments in the outer solar system with Voyager, P. IEEE, 75, 1404–1431, 1987.

Ware, R., Exner, M., Feng, D., Gorbunov, M., Hardy, K., Herman, B., Kuo, Y., Meehan, T., Melbourne, W., Rocken, C., Schreiner, W., Sokolovskiy, S., Solheim, F., Zou, X., Anthes, R., Businger, S., and Trenberth, K.: GPS sounding of the atmosphere from low Earth orbit: preliminary results, B. Am. Meteorol. Soc., 77, 19–40, 1996.

Wickert, J., Reigber, C., Beyerle, G., König, R., Marquardt, C., Schmidt, T., Grunwaldt, L., Galas, R., Meehan, T., Melbourne, W. G., and Hocke, K.: Atmosphere sounding by GPS radio occultation: first results from CHAMP, Geophys. Res. Lett., 28, 3263–3266, 2001.

Table 1. GNOS instrument parameters.

Parameter	Content
Constellation	GPS L1, L2
	Beidou B1, B2
Channel number	Positioning: 8
	Occultation: 6 (GPS)
	4 (Beidou)
Sampling rate	Positioning & Ionosphere occultation: 1 Hz
	Atmosphere occultation: CL 50 Hz
	OL 100 Hz
Output observations	TYPE: L1C, L2C, L2P/B1C, B2C
	CONTENTS: Pseudorange/carrier phase/SNR
Clock stability	1×10^{-12} (1secAllan)
Pseudorange precision	≤ 30 cm
Carrier phase precision	≤ 2 mm

Table 2. GNOS instrument characteristics.

	Occultation antenna (ROA and SOA)	Positioning antenna (PA)	Positioning RFU	Occultation RFU	EU
Number	2	1	1	2	1
Volume	600 × 135×12	135 × 120×7.5	100 × 80×30	182 × 105×108.7	240 × 180×130
Weight	≤ 2.0 kg×2	≤ 0.4 kg	0.4 kg	2.1 kg	5.0 kg
Total weight	≤ 14 kg				
Total power	≤ 40 W				

Fig. 1. GNOS instrument configuration.

Fig. 2. Global distribution of GNOS Beidou occultation events in 24 h simulation. Upward-pointing triangle triangles denote rising occultations. Downward-pointing triangles denote setting occultations.
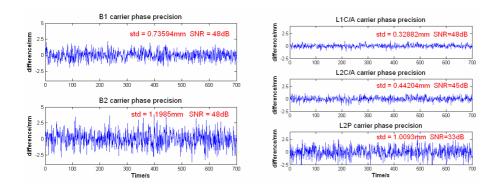
Fig. 3. Global distribution of GNOS GPS occultation events in 24 h simulation. Upward-pointing triangle triangles denote rising occultations. Downward-pointing triangles denote setting occultations.
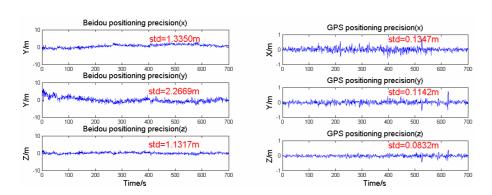
W. Bai et al.

Fig. 4. The example of GNOS pseudorange measurement precision for Beidou and GPS. The left panel shows the B1 and B2 peseudorange measurement precision. The right panel shows the L1C/A, L2C/A and L2P peseudorange measurement precision, respectively.
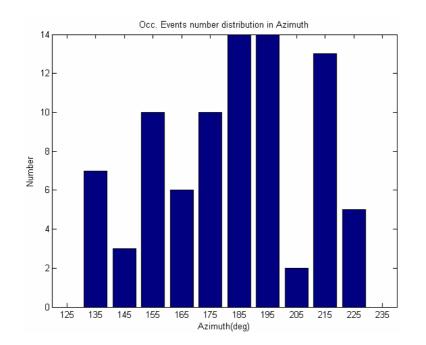
Fig. 5. Example of GNOS carrier phase measurement precision for Beidou and GPS. The left panel shows the B1 and B2 carrier phase measurement precision. The right panel shows the L1C/A, L2C/A and L2P carrier phase measurement precision.
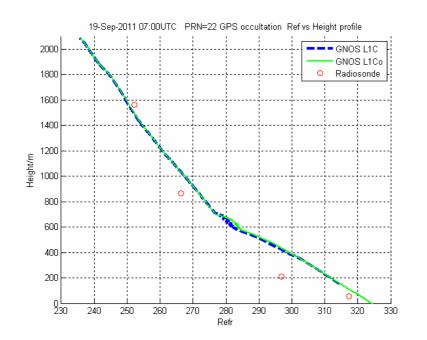
Fig. 6. Example of GNOS real-time navigation precision for Beidou and GPS. The left panel shows the Beidou navigation precision in three dimensions of WGS84 coordinates, the right panel shows the GPS navigation precision in there dimensions of WGS84 coordinates.
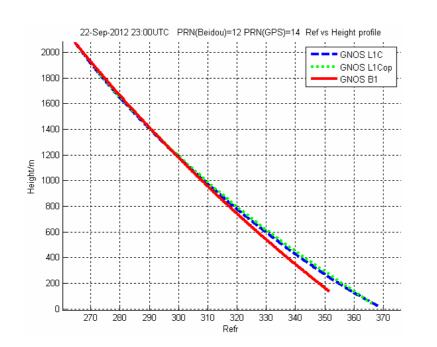
Fig. 7. Number of GNOS occultation events vs. azimuth in mountain-based experiment (21–25 September 2011).

Fig. 8. GPS occultation refractivity profile example (PRN = 22, 19 September 2011, 07:00 UTC). Blue dashed line donates the refractivity inverted from GNOS L1C/A CL data, green solid line donates the refractivity retrieved from GNOS L1C/A OL data, and red cycles denote the radiosonde data that took place with one hour in Beijing radiosonde station.

Fig. 9. GPS occultation refractivity profiles from Beidou (PRN = 12,MEO) and GPS (PRN = 14) on 22 September 2012 at 23:00 UTC). The blue dashed line donates the refractivity inverted from GNOS L1C/A CL data, the green dotted line donates the refractivity retrieved from GNOS L1C/A OL data, and the solid red line represents the refractivity obtained form GNOS B1 CL data. The two occultation events happened within half an hour.

Full Screen / Esc

Printer-friendly Version

Interactive Discussion